

RSC Advances



This is an *Accepted Manuscript*, which has been through the Royal Society of Chemistry peer review process and has been accepted for publication.

Accepted Manuscripts are published online shortly after acceptance, before technical editing, formatting and proof reading. Using this free service, authors can make their results available to the community, in citable form, before we publish the edited article. This *Accepted Manuscript* will be replaced by the edited, formatted and paginated article as soon as this is available.

You can find more information about *Accepted Manuscripts* in the [Information for Authors](#).

Please note that technical editing may introduce minor changes to the text and/or graphics, which may alter content. The journal's standard [Terms & Conditions](#) and the [Ethical guidelines](#) still apply. In no event shall the Royal Society of Chemistry be held responsible for any errors or omissions in this *Accepted Manuscript* or any consequences arising from the use of any information it contains.

ARTICLE

Hybrid Al₂O₃/Bio-TiO₂ Nanocomposite impregnated Thermoplastic polyurethane (TPU) nanofibrous membrane for Fluoride removal from aqueous solution

Cite this: DOI: 10.1039/x0xx00000x

Received 00th January 2012,
Accepted 00th January 2012

DOI: 10.1039/x0xx00000x

www.rsc.org/

S. P. Suriyaraj^a, Amitava Bhattacharyya^b, R. Selvakumar^{a*}

In the present study, crystalline TiO₂ nanoparticles were synthesized at room temperature using *Bacillus licheniformis* bacteria and further modified using alumina precursor to achieve hybrid biological and chemically synthesized Al₂O₃/TiO₂ nanocomposite. This hybrid nanocomposite was impregnated onto electrospun thermoplastic polyurethane (TPU) nanofibers. The adhesion of nanoparticles on nanofibers was achieved through silane functionalization of the materials. The HRTEM images confirmed proper impregnation of nanocomposite onto the nanofiber. The particle size and diameter of the nanocomposite and nanofiber were found to be 50±6 nm and 239±33 nm respectively. Other membrane parameters like thickness, swelling ratio and porosity were estimated. The nanocomposite impregnated nanofibrous membrane was tested for removal of fluoride from aqueous solution. The adsorption capacity (Q₀) of the nanocomposite impregnated TPU nanofiber was found to be 1.9 mg/g. This facile approach of designing nanocomposite impregnated nanofiber membrane can be used for water purification applications.

1. Introduction

In recent years, tailoring of polymeric nanofibers with functional nanomaterials has received immense curiosity leading to potential applications in the fields of water treatment, sensors, tissue engineering, drug delivery, catalyst, textiles, health care and various energy resources.¹⁻³ Among various applications, removal of various contaminants like fluoride, nitrate and sulphate from ground water has been seriously thought of.⁴

Various methods like chemical precipitation, electrocoagulation, reverse osmosis and electrodialysis have been reported to remove these contaminants from drinking water.⁵⁻⁶ Despite of unique advantages in these technologies, the cost factor, poor regeneration, interference of other ions, customary replacement of sacrificial electrodes, consumption of electric power, membrane fouling, requirement of experienced operators and poor water recoveries always remains a problem which has lead to limited social acceptance of these technologies. Scientific evidences recommend adsorption as the most efficient and cost effective method to remove contaminants like fluorides when compared to other methods.⁷⁻

⁸Among the various adsorbents reported, nanomaterials have been proved to have higher adsorption efficiency. Nanomaterials like alumina, titania, zinc oxide, magnesia, hydroxyapatite and its hybrid based nanocomposites are widely reported for fluoride removal. However the inability to recover nanomaterials after adsorption process is still a setback.⁹⁻¹⁰ Such particle recovery/ zero recovery ultimately leads to toxicological issue and add cost to the technology. In order to address this problem scientists have tried to immobilize/impregnate nanomaterials on to various support matrix. Few support matrix reported in literature are nanofibers, porous ceramics, microorganism etc.¹¹ Among the support matrix, nanofibers are considered to be effective in terms of charged surface area, easy synthesis process and possibility of surface modification.¹²⁻¹³ Various polymers like polyurethane (PU), polyacrylonitrile (PAN), poly (vinyl alcohol) (PVA), poly (acrylic acid) (PAA) and cellulose based membranes have been used for synthesis of nanofibers.¹⁴ Among them, polyurethane has been extensively used for the water filtration systems due to its immense properties like oil/solvent resistance, abrasion resistance, weather (UV) resistance, high-temperature resistance and enhanced mechanical properties.¹⁵⁻¹⁶

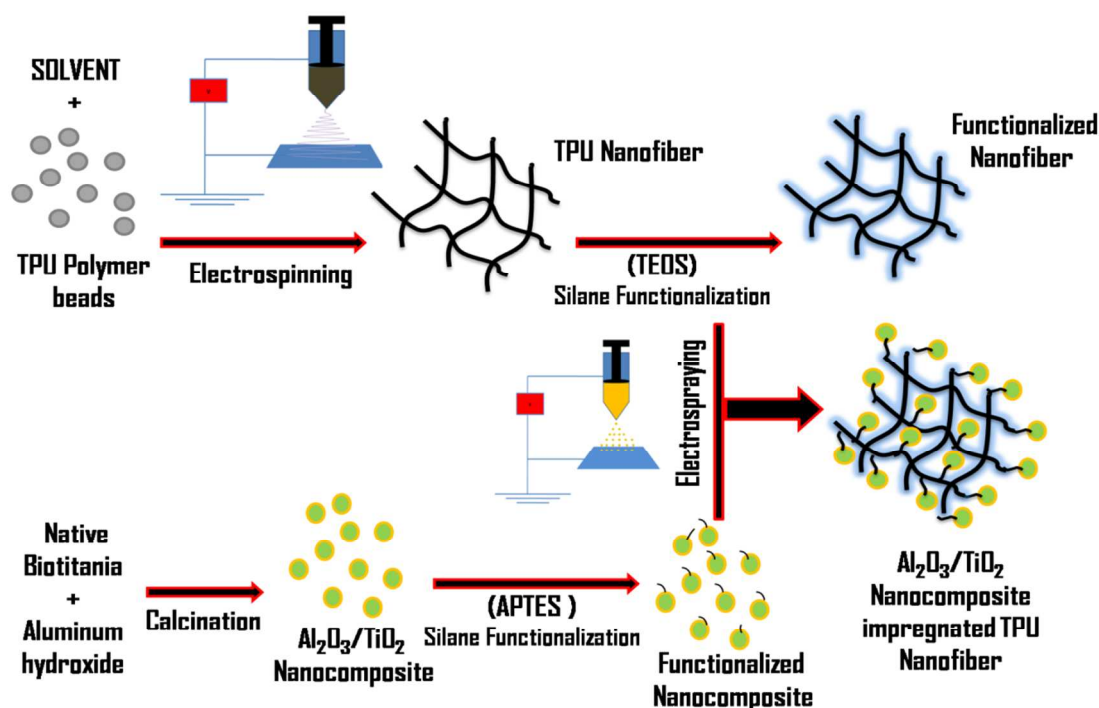


Fig. 1: Schematic representation of the preparation of $\text{Al}_2\text{O}_3/\text{Bio-TiO}_2$ nanocomposite impregnated TPU nanofiber

In order to introduce nanomaterials onto the nanofibrous membrane, various methods like blending, dip coating, surface nucleation and hot press have been adopted and each of these techniques meets some disadvantages in water treatment.^{17,14} It is difficult to achieve sufficient exposure to adsorbate for the polymer blended nanoparticles since the nanoparticles are surrounded by polymers leading to decrease in interaction between the nanomaterials and adsorbate. The surface nucleation method needs high temperature to make nanomaterials more crystalline and activated. The post temperature treatment in case of surface nucleation is not possible in temperature-sensitive substances like polymers. Hence the surface functionalization of the active nanoparticles or nanofibers with suitable adhesive functional materials like silane would be more suitable for the impregnation of nanoparticles onto the nanofibers.¹⁸

These nanoparticle impregnated hybrid nanofibers have unique and interesting features, such as high surface area to volume ratio, large porosity, good mechanical properties, good water permeability and increased elution quality due to complete solid/liquid separation, that makes them suitable for water treatment.^{12,17} However there are very few reports on the nanoparticle based nanofiber membranes for fluoride removal.^{4,6} In the present study, we have exploited the fluoride adsorption property of $\text{Al}_2\text{O}_3/\text{Bio-TiO}_2$ nanocomposite (ABN) and $\text{Al}_2\text{O}_3/\text{Bio-TiO}_2$ nanocomposite impregnated electrospun TPU nanofiber membrane (ABN/TPU-NFM) for water purification. The nanocomposite, nanofiber and nanocomposite impregnated nanofibers were characterized using XRD, FE-

SEM, HR-TEM and FTIR. The experimental data were fitted onto suitable isotherm and kinetics.

2. Experimental section

2.1. Materials

Titanium and aluminum precursor (purity > 99.9%), were purchased from Sigma Aldrich, India. The media supplements such as $\text{Na}_2\text{HPO}_4 \cdot 7\text{H}_2\text{O}$ (purity > 99%), KH_2PO_4 (purity > 99%), NaCl (purity > 99%), NH_4Cl (purity > 99%) and Glucose (purity = 99%), were purchased from Himedia, India. N, N-dimethylformamide, tetraethyl orthosilicate (TEOS) and (3-Aminopropyl)triethoxysilane (APTES) were purchased from Merck, India. Texin 945 U grade TPU was supplied from Bayer Material Science. 1, 2-cyclohexane diaminetetraacetic acid based total ionic strength adjustment buffer (TISAB) was purchased from Thermo Scientific, USA. All chemicals were used without further purification. Millipore ultra pure water was used throughout the experiment.

2.2. Preparation of TPU nanofiber

The TPU nanofiber was prepared by electrospinning process.³ In brief, the polymer solution was prepared by dissolving 1 g of TPU in a solvent containing N, N-Dimethylformamide and acetone in the ratio of 7:3 (v/v) followed by heating at 80 °C on a hot plate with vigorous stirring. The prepared polymeric solution was electrospun (Electrospinning Unit, PSGIAS, India) onto aluminum plate. The nanofibers were electrospun using a current supply of 30 kV, working distance of 18.5 cm using

syringe needle (20 gauge) at a flow rate of 0.7 mL/h. The collection time was kept as 2 h.

2.3. Preparation of ABN

The synthesis and characterization of biotitania were already reported in our previous paper.¹⁹ The biologically synthesized titania nanoparticles was modified using aluminum precursor to produce ABN. In brief, 0.25 g of native biotitania was well dispersed in 10 mL of Millipore water and mixed with 7.5% aluminum hydroxide solution. The mixture was continuously stirred for 15 min. Then sample was dried at room temperature and calcined at 700 °C for 1 h. The calcined nanocomposite was stored at room temperature and used for further studies.

2.4. Preparation of ABN/TPU-NFM

The impregnation of the nanocomposite material onto the nanofiber was done using silane functionalization of both fiber and nanocomposite surfaces.¹⁸ Initially the nanofibers were surface functionalized using tetraethyl orthosilicate (TEOS) silica solution to increase the surface adhesive property. Further the nanocomposite suspension was prepared by rapidly stirring 1 g of nanocomposite in 10 mL of 50% ethanol followed by adding APTES to the mixture. After stirring, the nanocomposite suspension was electrosprayed on to the functionalized TPU nanofibers using the following parameters. Current supply of 30 kV, 10 cm working distance, 20 gauge syringe needle, 3 mL/h flow rate and the collection time was set to 1 h. The nanocomposite impregnated TPU nanofibers were dried at 37 °C for 1 h and used for further study. The schematic representation of the preparation of ABN/TPU-NFM is shown in Fig. 1.

2.5. Characterization

The phase identification and crystal structures of the ABN and ABN/TPU-NFM were characterized by the XRD technique using X-ray diffractometer (XRD- 600, Shimadzu, Japan) having CuK α radiation, $\alpha = 1.54 \text{ \AA}$ with generator settings of 30 mA; 40 kV; step size 0.05 (2 θ) with scan step time of 10.16 seconds in continuous mode. HR-TEM images were taken in JEOL- JEM 2100 (Japan) with an accelerating voltage of 80 kV for nanofibers and nanocomposite impregnated nanofibers and 200 kV for nanocomposite. The selected area electron diffraction (SAED) of the membrane and composite material was performed. The morphology of the nanofibers was characterized using FE-SEM (SEM JEOL-JSM 6390, Japan) and images were captured at an accelerating voltage of 10 kV for control TPU nanofibers and 20 kV for ABN/TPU-NFM. In order to evaluate the elemental composition of the nanofibers and nanocomposite impregnated nanofibers, EDS technique was applied to corresponding FE-SEM image. The FTIR spectroscopy was carried out for surface functional group analysis using a Nicolet Avathar- 320 FTIR spectrometer (Nicolet Instruments, Madison) at a scan range of 4000-400 cm⁻¹ with a scanning speed of 2mm/sec. Membrane properties such as membrane thickness, swelling ratio and porosity of the nanofiber have been studied according to Vasconcelos et al.²⁰

2.6. Estimation of fluoride

Fluoride estimation was performed using Thermo Scientific Orion four star ion selective electrode meter, USA according to ASTM D 1179 standards. The electrode was calibrated using standard fluoride concentrations in the range of 0.1–10 mg/L and set as the minimum detection limit of 0.1 mg/L for fluoride testing. 1, 2- cyclohexane diaminetetraacetic acid (CDTA) was used as a total ionic strength adjustment buffer reagent thought the experiment.

2.7. Adsorption studies

The synthesized ABN and ABN/TPU-NFM were used as adsorbent materials for the removal of fluoride from aqueous solution. Experiments were conducted by simple batch mode adsorption for the ABN and dip mode adsorption method for ABN/TPU-NFM. Batch mode studies were carried out by agitating 0.2 g of ABN in 200 mL of F⁻ solution of desired concentration and pH at 120 rpm at room temperature. The flasks were withdrawn at predetermined time intervals. The adsorbate concentration in the supernatant was determined. In case of ABN/TPU-NFM, the experiments were carried out using simple dip mode adsorption method. Various concentrations of the adsorbate (2–10 mg/L of F⁻, respectively) were taken in plastic flasks and dipped with 8 cm²/200 mL of membrane material. The samples were withdrawn at predetermined time intervals and estimated. Control experiments were carried out without adsorbent to estimate the adsorption of fluorides on to the flasks. Similarly, the studies were carried out with varying membrane size (1, 2, 3, 4 and 8 cm²) in 200 mL of F⁻ solution of desired concentration and pH at room temperature.

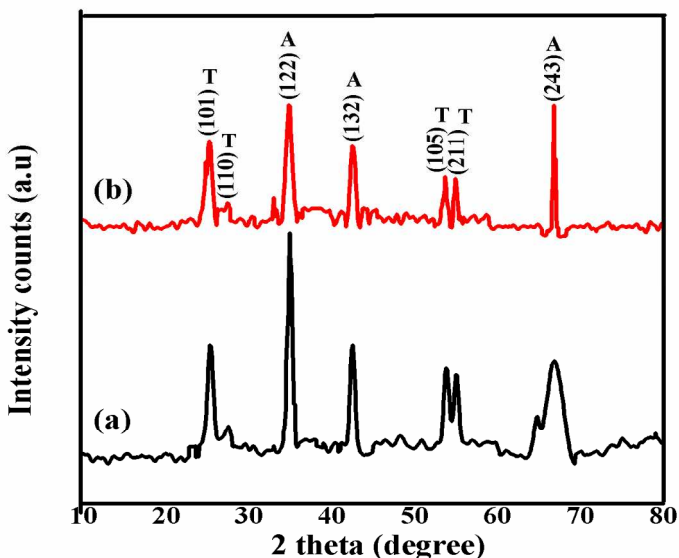


Fig. 2 XRD pattern of Al₂O₃/TiO₂ nanocomposite (a) and nanocomposite impregnated TPU nanofiber (b)

The adsorption percentage was determined using Equation 1.

$$\text{Percentage F}^- \text{ removal} = (C_i - C_f) / C_i \times 100 \quad (1)$$

where C_i is the initial adsorbate concentration and C_f is final adsorbate concentration. The adsorption kinetics (Pseudo first order and second order) and Langmuir isotherm were employed to study the adsorption efficiency.

3. Results and discussion

The properties of the control TPU nanofiber and ABN/TPU-NFM are tabulated in the supplementary Table S1.

3.1. Characterization

X-ray diffraction patterns of ABN and ABN/TPU-NFM are shown in Fig. 2. In Fig. 2 (a) the alumina peak showed maximum intensity and confirmed that the alumina ratio was higher than titania in the nanocomposite. The intensity peaks (122, 132 and 243) corresponded to the orthorhombic crystal structure of alumina with space group $pnm2_1$ (33) and cell dimensions $a = 4.843 \text{ \AA}$, $b = 8.330 \text{ \AA}$ and $c = 8.954 \text{ \AA}$ (JCPDS card no 88-0107). The intensity peaks (101, 105 and 211) corresponded to anatase phase having a body centred tetragonal crystal structure of titania with space group $I4_1/amd$ (no. 141) and cell dimensions $a = 3.758 \text{ \AA}$ and $c = 9.513 \text{ \AA}$ (JCPDS card no 21-1272). The presence of similar peaks was observed in the Fig. 2 (b) which indicates the presence of ABN onto the polymer nanofibers. The control TPU does not show any peaks under XRD as it is pseudo-crystalline in nature (Supplementary Fig. S1). The control TPU nanofiber and $\text{Al}_2\text{O}_3/\text{TiO}_2$ impregnated nanofiber were studied using FE-SEM. Fig. 3(a) clearly indicates the formation of TPU nanofibers. The control TPU nanofibers were smooth and continuous with an average diameter of $239 \pm 33 \text{ nm}$.

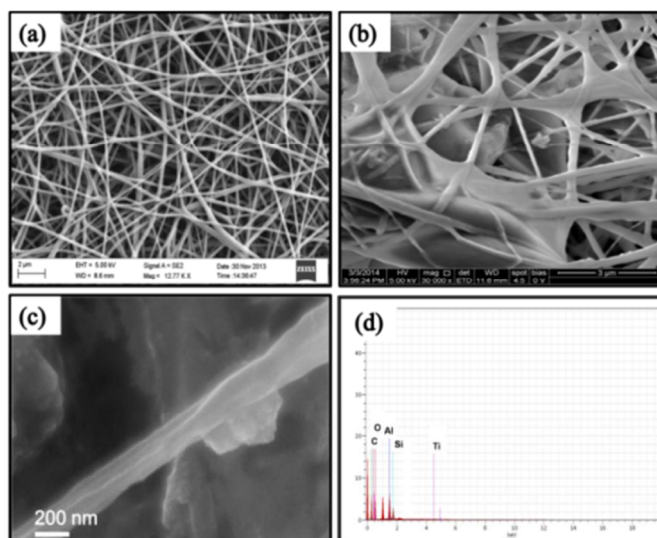


Fig. 3 FE-SEM image of control TPU nanofibers (a) ABN/TPU-NFM (b) and its respective high resolution image (c) corresponding EDS spectrum (d)

The functionalized TPU nanofiber did not show any major variation in fiber diameter when compare to control. Once the functionalized ABN was electro sprayed, the particles got deposited onto the functionalized nanofibers. The magnified image of the impregnated nanocomposite material on to the nanofiber is shown in the Fig. 3 (b and c). The silane functionalization of the surface of nanocomposites as well as nanofibers facilitates uniform impregnation. Similar reports like functionalization of gold nanoparticles using silane groups and the adherence of functionalised nanoparticles onto the nanofibers were performed by McCann et al.¹⁶ The EDS spectra confirmed the presence of Al, Ti and O from the nanocomposite, Si from silane and C from the polymer of the corresponding FESEM image (Fig. 3 (d)).

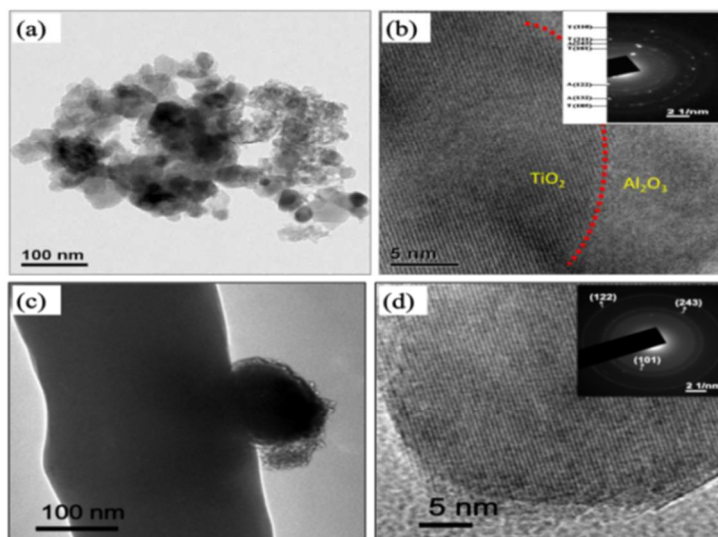


Fig. 4 HRTEM image of ABN (a) and its respective high resolution image (b) and SAED pattern (b insert). ABN/TPU-NFM (c) its respective high resolution image (d) and SAED pattern (d insert)

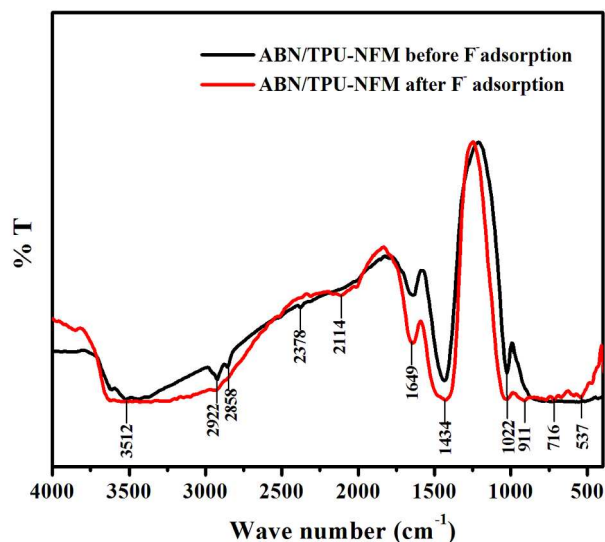


Fig. 5 FTIR spectra of ABN/TPU-NFM before and after fluoride adsorption

The morphology and crystalline nature of the nanocomposite was imaged using HRTEM. Fig. 4a shows that the alumina was evenly distributed on the surface of crystalline biotitania nanoparticles. The particle size of the nanocomposite was found to be 50 ± 6 nm. The high resolution image of the nanocomposite clearly indicated the difference in atomic arrangements of alumina and biotitania within the same nanocomposite (Fig. 4b). The HR-TEM image of prepared ABN/TPU-NFM is shown in Fig. 4(c). The image reveals the proper impregnation of the nanocomposite material onto the smooth TPU nanofibers. The high resolution image of the nanocomposite present onto the fibers shows similar crystalline nature (Fig. 4b). The SAED patterns (Fig. 4b and 4d insert) of ABN and ABN/TPU-NFM were in agreement with the corresponding XRD data. The FTIR spectra (Fig. 5) of the ABN/TPU-NFM showed characteristic band at 3512 cm^{-1} assigned to surface OH group represents either the uncondensed silanol group or the $-\text{OH}$ group in the water or alcohol liberated due to the condensation reactions of TEOS.²¹ The bands at 2922 and 2858 cm^{-1} can be attributed to asymmetric and symmetric stretching of CH_2 group.²² The characteristic bands at 2378 and 2114 cm^{-1} was due to atmospheric CO_2 asymmetrical stretching vibration.²³ The band at 1649 cm^{-1} attributed to the stretching of $\text{C}=\text{O}$ of urethane and 1434 and 1022 cm^{-1} corresponds to the $\text{Si}-\text{O}$ and $\text{Si}-\text{O}-\text{R}$ groups present in the nanocomposite and the nanofiber membranes.²⁴ The adsorption peak at 911 cm^{-1} is due to the vibration of $\text{Ti}-\text{O}-\text{Si}$ or $\text{Al}-\text{O}-\text{Si}$.²⁵

3.2. Adsorption of F^- using ABN and ABN/TPU-NFM

3.2.1. Effect of contact time and initial concentration on F^- adsorption

The contact time (the time taken by the adsorbent to complete the adsorption after which the saturation occurs) between the adsorbate and adsorbent plays a significant role for

the removal of fluoride from aqueous solution during batch mode and dip mode adsorption studies. In batch mode adsorption of fluoride using ABN, the fluoride uptake was found to increase with contact time and remained constant after equilibrium. The contact time varied from 20 to 30 min as the concentration of fluoride increased from 2 – 10 mg/L. The maximum F^- removal was observed up to 72.8% in low adsorbate concentration of 2 mg/L and the percentage removal constantly reduced up to 25.6% as the concentration was increased to 10 mg/L (Supplementary Fig. S2). This showed that fluoride removal capacity was reduced while increasing the adsorbate concentration. Similarly, In case of dip mode adsorption studies, the F^- uptake was found to increase with contact time and remained constant after equilibrium. The contact time varied from 20 to 40 min as the concentration of fluoride increased from 2 – 10 mg/L (Fig. 6). The pictorial representation of the removal of fluoride using ABN/TPU-NFM by dip mode adsorption is shown in the Fig. 7. The initial rapid phase of adsorption may be due to the availability of a large number of active sites on the adsorbent surface.²⁶ The percentage F^- removal was found to be 93% for the initial F^- concentration of 2 mg/L and further decreased from 93% to 19%, as the initial F^- concentration increased from 2 to 10 mg/L. The change in the percentage removal might be due to the fact that initially all adsorbent sites were vacant and the solute concentration gradient was high. Later, the fluoride uptake rate by adsorbent had decreased significantly due to the decrease in number of adsorption sites.²⁷ Suriyaraj et al.²⁶ obtained 74.6% of F^- adsorption using biotitania nanoparticles within contact time of 80 min. Similarly iron and aluminum based mixed hydroxides required an equilibrium time of 2 h for the adsorption of fluoride.²⁸ When compared to these studies, our nanocomposite impregnated TPU nanofiber was found to be much superior in adsorbing 93% of F^- within 30 min of contact time at an initial concentration of 2 mg/L.

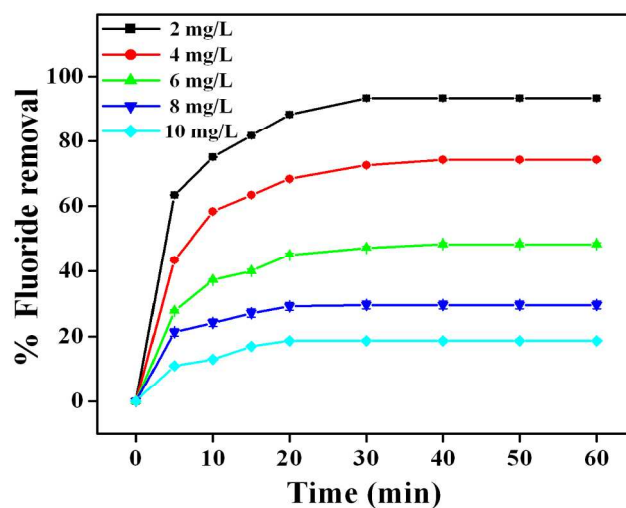


Fig. 6 Effect of contact time and initial concentration on F^- adsorption by ABN/TPU-NFM (Membrane size: 8 cm^2 ; pH: 7 and temp: $30 \pm 2 \text{ }^\circ\text{C}$)

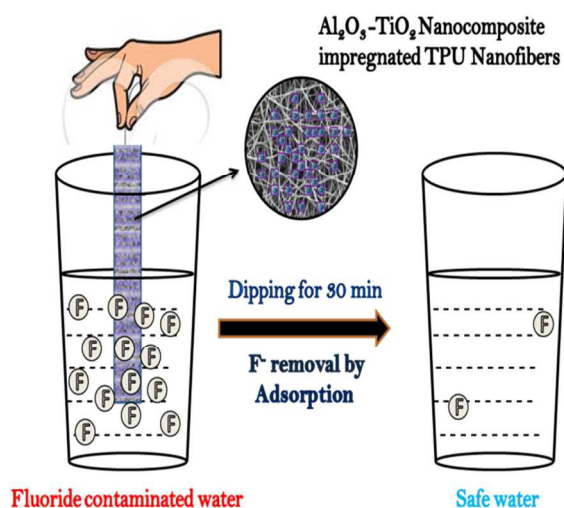


Fig.7 Pictorial representation of working method of ABN/TPU-NFM for fluoride adsorption

3.2.2. Effect of the varying membrane size on F⁻ adsorption

The impact of varying ABN/TPU-NFM size on F⁻ adsorption was studied using a constant fluoride concentration of 6 mg/L. The pH of the solution was maintained at neutral. The results obtained are shown in Fig. 8. With increase in the nanofiber size from 1 – 8 cm², the percentage fluoride removal also increased from 11% to 48%. The availability of more nanocomposite and area for interaction of the adsorbent could be the reason for the increase in percent removal of adsorbate with the increase in membrane size.²⁶

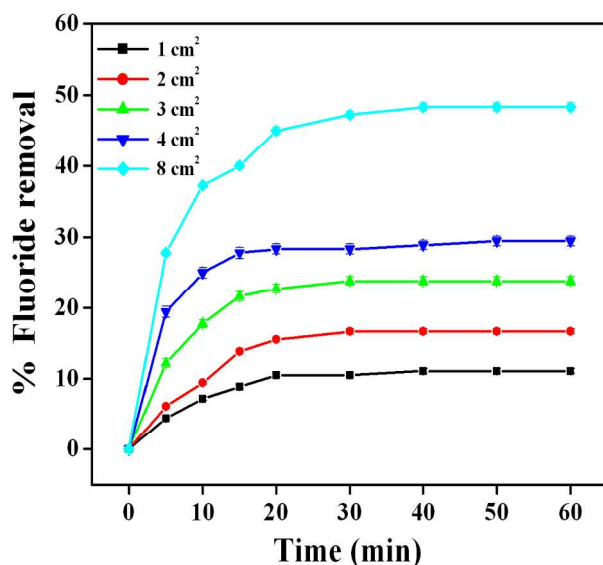


Fig. 8 Effect of the membrane size on F⁻ adsorption (Adsorbate concentration: 6 mg/L; pH: 7; temp: 30±2 °C)

3.3. Adsorption Kinetics

A study of adsorption kinetics is desirable as it provides information about the rate of the reaction, which is important to determine the efficiency of the process. The rate constant of adsorption is determined from the first order rate expression given by Lagergren and Svenska (1898).²⁹The pseudo-first-order equation can be written as:

$$dq_t/dt = k_1(q_e - q_t) \quad (2)$$

Integrating this for the boundary conditions $t = 0$ to $t = t$ and $q_t = 0$ to $q_t = q_t$, gives

$$\ln(1 - q_t/q_e) = -k_1 t \quad (3)$$

where k_1 is the rate constant (h^{-1}), q_e (mg/g) is the amount of solute adsorbed on the surface at equilibrium, q_t (mg/g) is the amount of solute adsorbed at any time t .

Pseudo-second-order equation (Ho and McKay1998)³⁰ based on equilibrium adsorption can be expressed as:

$$1/q_t - 1/q_e = 1/k_2 q_e^2 t \quad (4)$$

where k_2 (g/mg h) is the pseudo-second-order rate constant. Both k_1 and k_2 values can be calculated from the slopes of the plots $\ln(1 - q_t/q_e)$ versus t and $1/q_t - 1/q_e$ versus $1/t$, respectively.

The k_1 and k_2 values were obtained from the slopes of the plots $\ln(1 - q_t/q_e)$ versus t for pseudo-first order model and $1/q_t - 1/q_e$ versus $1/t$ for pseudo-second order model, respectively. The parameters of the pseudo-first-order and pseudo second order models of ABN/TPU-NFM are summarized in Table 1 which shows the comparison of adsorption kinetics data for both models with different initial F⁻ concentrations. The results of fitting first order and second order kinetic model data for the fluoride adsorption by ABN are presented in Supplementary Table 1. The values of the coefficient of determination (R^2) clearly indicate that the experimental data are in good agreement with second order kinetic model. This shows that the mechanism of the adsorption can be described by the pseudo second order kinetic model, based on the assumption that the rate-limiting step may be chemisorptions involving valence forces through sharing or exchange of electrons between the nanocomposite on to the fibers and pollutant ions. The experimental q_e value and the calculated q_e values were matching with pseudo second order kinetic and failed to obey pseudo first order kinetics.

Table 1 First order and second order kinetics for F⁻ adsorption by ABN/TPU-NFM

Initial F ⁻ conc (mg/L)	q _e (exp) (mg/g)	First order kinetic model			Second order kinetic model		
		k ₁ (L/min)	q _e (cal) (mg/g)	R ²	k ₂ (g/mg/min)	q _e (cal) (mg/g)	R ²
2.0	1.867	0.136	1.534	0.971	0.812	1.742	0.996
4.0	2.967	0.120	2.529	0.991	3.033	2.817	0.996
6.0	2.9	0.122	2.576	0.989	2.789	2.770	0.996
8.0	2.367	0.193	2.376	0.951	1.749	2.183	0.995
10.0	1.867	0.150	1.879	0.952	0.779	1.773	0.991

Table 2 Summary of the Maximum F⁻ removal capacities by different adsorbents

S. no	Adsorbent	Adsorption capacity mg/g	Reference
1	Activated silica gel	0.244	[32]
2	Modified natural zeolite	1.766	[33]
3	AIC-300 carbon	1.1	[34]
4	Activated alumina	1.45	[35]
5	Aluminium impregnated chitosan (AIC)	1.73	[36]
6	Aluminium-Cerium-Calcium-Alginate composite	1.438	[37]
7	Hydroxyapatite	1.432	[38]
8	Magnesium Titanate	0.03	[39]
9	Biotitania	0.85	[26]
10	ABN	2.73	Present study
11	ABN/TPU-NFM	1.9	Present study

3.4. Adsorption isotherm

Langmuir adsorption isotherm for the fluoride adsorption by ABN and ABN/TPU-NFM was used to analyze equilibrium adsorption data. The isotherm is represented by the following equation (5).

$$Q_0 = q_e (1 + bC_e) / bC_e \quad (5)$$

where C_e is the equilibrium concentration (mg adsorbate per litre of solution) and q_e is the amount adsorbed (mg adsorbate per g of adsorbent) at equilibrium.³¹ The constant Q_0 signifies the monolayer adsorption capacity (mg/g) and b is Langmuir constant. Plots of q_e vs. C_e show the agreement of experimental data with Langmuir plot for F⁻ removal using synthesized adsorbent materials. The maximum adsorption capacity (Q_0) of the ABN and ABN/TPU-NFM adsorbent materials (Fig. 9) was found to be 2.73 and 1.9 mg/g. The fluoride adsorption capacity of the adsorbents developed in the present study was higher than that of the other reported values in literature (Table 2).

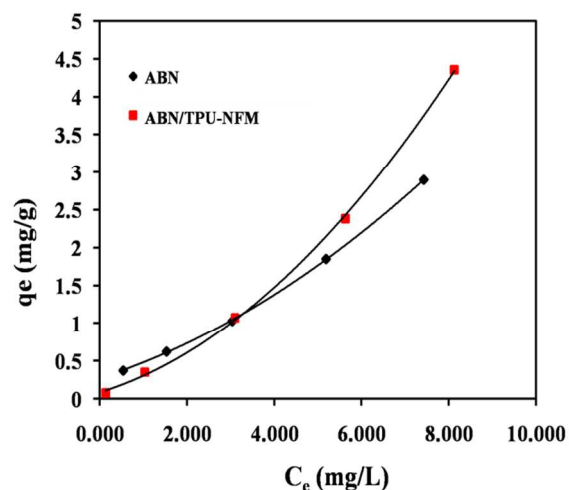
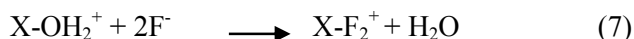
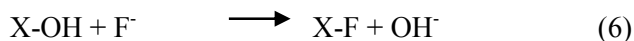


Fig. 9 Langmuir isotherm model for fluoride adsorption by ABN and ABN/TPU-NFM

3.5. Mechanism of F⁻ adsorption

The adsorption of fluoride onto nanocomposite adsorbent used in the present study can be explained by the formation of surface complexes according to the following equation.



where, X is the surface functional group of the (Al/Ti) metal oxide on nanofiber surfaces. The extent of adsorption is limited to the number of exchangeable surface hydroxyl groups, which is a function of surface area. All adsorbing species, including protons compete for favourable surface sites present on the nanocomposite adsorbent.²⁶ The FTIR spectra of nanocomposite adsorbent after fluoride adsorption shows that the functional hydroxyl groups were involved in the adsorption reaction and band shift from 1022 cm⁻¹ to 716 and 537 cm⁻¹ was observed (Fig. 5). Such band shift is due to the hydroxide bridging between fluoride ions and the metal oxide surfaces.⁴⁰ The intensity of the O-H band decreases in after fluoride adsorption and this showed that the surface hydroxyl groups of nanocomposite present on to the nanofibers were involved in the fluoride adsorption.²⁶

4. Conclusions

In summary, the synthesized ABN was impregnated on the electrospun TPU nanofibers using silane functionalization and simple electrospaying approach. The impregnated membrane was tested for fluoride removal using simple dip mode adsorption method. We observed that the ABN/TPU-NFM was having the potential to adsorb fluoride from aqueous solution. The maximum adsorption capacity (Q₀) of the adsorbent was found to be 1.9 mg/g. The adsorption kinetic process obeys pseudo second order kinetic and failed to obey pseudo first order kinetic models. The experimental data clearly indicate the possible application of the developed Al₂O₃/Bio-TiO₂ nanocomposite impregnated TPU nanofiber in removal of fluoride from drinking water through a simple dipping process which is easy to use than other reported techniques.

Acknowledgements

The authors are thankful to Life Science Research Board (DRDO-LSRB) (Sanction No: LSRB-235/BTB/2011), Govt of India, for funding the work. The authors also thank Uranium Corporation of India Limited (UCIL) for providing ore samples. Support and help rendered by PSG Management and PSG Institute of Advanced Studies is acknowledged. The authors are thankful to Bayer Material Science for providing polymers.

Notes and references

^aNanobiotechnology laboratory, PSG Institute of Advanced Studies, P.B. No: 1609, Peelamedu, Coimbatore 641004, India. Tel.: +91 422 4344000 extn 4321; E-mail: selvabiotech@gmail.com, rsk@ias.psgtech.ac.in

^bAdvanced Textile and Polymer Research Laboratory, Nanotech Research Facility, PSG Institute of Advanced Studies, Peelamedu, Coimbatore 641004, India

1. L. M. Colangelo, A. J. Baumner, *Anal. Chem.*, 2014, 7, 23.
2. R. Sahay, P. Suresh Kumar, R. Sridhar, J. Sundaramurthy, J. Venugopal, S. G. Mhaisalkar and S. Ramakrishna, *J. Mater. Chem.*, 2012, 22, 12953.
3. R. Selvakumar, S. N. M. Mohaideen S. Aravindh, C. Sabarinath, M. Ananthasubramanian, *J Membrane Biol.*, 2014, 247, 35.
4. A. Mahapatra, B. G. Mishra, G. Hota, *Ind. Eng. Chem. Res.*, 2013, 52, 1554.
5. S. Mohapatra, S. Anand, B. K. Mishra, D. E. Giles, P. Singh. *J Environ Manage*, 2009, 91, 67.
6. A. Bhatnagar, E. Kumar, M. Sillanpaa, *Chem Eng J.*, 2011, 171, 2011, 811.
7. S. Ayoob, A. K. Gupta, T. Venugopal, A. Bhat, *Environ. Sci. Technol.*, 2008, 38, 401.
8. S. Jagtap, M. K. Yenkie, N. Labhsetwar and S. Rayalu, *Chem. Rev.*, 2012, 112, 2454.
9. V. Tomar and Dinesh Kumar, *Chem Cent.*, 2013 7, 51.
10. L. Srivastav, Prabhat K. Singh, V. Srivastava, C. Yogesh, Sharma, *J Hazard Mater.*, 2013, 2639, 342.
11. T. Pradeep and Anshup, *Thin Solid Films.*, 2009, 517, 6441.
12. M. Botes and T. Eugene Cloete, *Crit Rev Microbiol.*, 2010, 36, 68.
13. M. T. Amin, A. A. Alazba, and U. Manzoor, *Adv. Mater. Sci. Eng.*, 2014, 1.
14. S. Homaeigohar, M. Elbahri, *Materials.*, 2014, 7, 1017.
15. M. Aurilia, F. Piscitelli, L. Sorrentino, M. Lavorgna, S. Iannace, *Eur. Polym. J.*, 2011, 47, 925.
16. A. Bhattacharyya, K. Karthikeyan, J. Mangala, *Nanosci and Nanotech. Lett.*, 2014, 6, 438.
17. S. P. Suriyaraj, B.M. Benasir, S. G. Deepika, P. Biji, R. Selvakumar, *Water Sci. & Tech.: Water Supp.*, 2014, 14, 554.
18. B. Y. Lee, K. Behler, M. E. Kurtoglu, Meghan, A. Wynosky-Dolfi, Richard F. Rest, Y. Gogotsi, *J Nanopart Res.*, 2010, 12, 2511.
19. S. P. Suriyaraj, R. Selvakumar, *RSC Adv.*, 2014, 4, 39619.
20. A. Vasconcelos, A. C. Gomes, A. C. Paulo, *Acta Biomaterialia.*, 2012, 8, 3049.
21. P. A. Patel, J. Eckart, M. C. Advincula, A. J. Goldberg, P. T. Mather, *Polymer.*, 2009, 50, 1214.
22. S. Devaraju, P. Prabunathan, M. Selvi, M. Alagar, *Front Chem.*, 2013, 1: 19.
23. H. Pan, X. D. Wang, S.S.Xiao, L. G. YU, Z. J. Zhang *Indian J Eng Mater S.*, 2013, 20, 561.

24. G. H. Lopes, J. Junges, R. Fiorio, M. Zeni, A. J. Zattera, *Mater. Res.*, 2012, 15, 698.
25. M. Riazian, N. Montazeri, E. Biazar, *Orient J Chem.* 2011, 27, 903.
26. S. P. Suriyaraj, T. Vijayaraghavan, P. Biji, R. Selvakumar, *J. Environ. Chem. Eng.*, 2014, 2, 444.
27. R. Selvakumar, N. Arul Jothi, V. Jayavignesh, K. Karthikaiselvi, G. Antony, P. R. Sharmila, S. Kavitha, K. Swaminathan, *Water Res.*, 2011, 45, 583.
28. M. G. Sujana, G. Soma, N. Vasumathi, S. Anand, *J Fluorine Chem.*, 2009, 130, 749.
29. S. Langergren, K. Svenska, *Vetenskapsad Handl.*, 1898, 24, 1.
30. Y.S. Ho, G. McKay, *Process Biochem.*, 1999, 34, 451.
31. I. Langmuir, *J. Am. Chem. Soc.*, 1918, 40, 1361.
32. N. K. Mondal, R. Bhaumik, A. Banerjee, J. K. Datta, T. Baur, *Inter. J. Environ. Sci.*, 2012, 2.
33. Z. Zhang, Y. Tan, M. Zhong, *Desalination.*, 2011, 276, 246.
34. R. L. Ramos, J. Ovalle-Turrubiartes and M. Sanchez-Castillo, *Carbon.*, 1999, 37, 609.
35. S. Ghorai, K. K. Pant, *Sep Purif Technol.*, 2005, 42, 265.
36. S. K. Swain, R. K. Dey, M. Islam, R. K. Patel, U. Jha, T. Patnaik and C. Airoidi, *Sep. Sci Technol.*, 2009, 44.
37. S. K. Swain, T. Patnaik and R. K. Dey, *Desalination Water Treat.*, 2013, 51, 22.
38. S. Gao, R. Sun, Z. Wei, H. Zhao, H. Li, F. Hu, , *J Fluorine Chem.*, 2009, 130, 550.
39. V. Gopal, K. P. Elango, *Indian J Chem Technol.*, 17, 28.
40. K. Biswas, S. K. Saha, U. C. Ghosh, *Ind. Eng. Chem. Res.*, 2007, 46, 5346.